Environmental Pollution 245 (2019) 77–88

Contents lists available at ScienceDirect

Environmental Pollution

journal homepage: www.elsevier.com/locate/envpol

Vertical mixing with return irrigation water the cause of arsenic enrichment in groundwater of district Larkana Sindh, Pakistan☆

Waqar Ali [a, b, c], Nisbah Mushtaq [a], Tariq Javed [e], Hua Zhang [b], Kamran Ali [d], Atta Rasool [a, b], Abida Farooqi [a, *]

[a] Hydro Geochemistry Laboratory, Department of Environmental Sciences, Faculty of Biological Sciences, Quaid-I-Azam University, Islamabad, PO, 45320, Pakistan
[b] State Key Laboratory of Environmental Geochemistry, Institute of Geochemistry, Chinese Academy of Sciences, Guiyang, 550081, China
[c] University of Chinese Academy of Sciences, Beijing, 100049, China
[d] Institute of Environmental Sciences and Engineering (IESE), School of Civil and Environmental Engineering (SCEE), National University of Science and Technology (NUST) Islamabad, Pakistan
[e] Isotope Application Division, Pakistan Institute of Nuclear Science and Technology (PINSTECH), Nilore, Islamabad, Pakistan

ARTICLE INFO

Article history:
Received 6 June 2018
Received in revised form
3 October 2018
Accepted 23 October 2018
Available online 29 October 2018

Keywords:
Arsenic
Isotopes
Saturation indices
Vertical mixing
Return irrigation

ABSTRACT

Stable isotopes ratios (‰) of Hydrogen (δ^2H) and Oxygen ($\delta^{18}O$) were used to trace the groundwater recharge mechanism and geochemistry of arsenic (As) contamination in groundwater from four selected sites (Larkana, Naudero, Ghari Khuda Buksh and Dokri) of Larkana district. The stable isotope values of δ^2H and $\delta^{18}O$ range from 70.78‰ to −56.01‰ and from −10.92‰ to −7.35‰, relative to Vienna Standard for Mean Ocean Water (VSMOW) respectively, in all groundwater samples, thus indicating the recharge source of groundwater from high-salinity older water. The concentrations of As in all groundwater samples were ranged from 2 μg/L to 318 μg/L, with 67% of samples exhibited As levels exceeding than that of World Health Organization (WHO) permissible limit 10 μg/L and 42% of samples expressed the As level exceeding than that of the National Environmental Quality Standard (NEQS) 50 μg/L. The leaching and vertical mixing with return irrigation water are probably the main processes controlling the enrichment of As in groundwater of Larkana, Naudero, Ghari Khuda Buksh and Dokri. The weathering of minerals mostly controlled the overall groundwater chemistry; rock-water interactions and silicate weathering generated yielded solutions that were saturated in calcite and dolomite in two areas while halite dissolution is prominent with high As area.

1. .Introduction

Arsenic (As) is one of the most toxic and carcinogenic contaminants in groundwater. The WHO and United State Environment Protection Agency (USEPA) have defined the maximum permissible limit of As in groundwater as 10 μg/L (Hassan et al., 2009). However, many developing countries have permissible As contamination limits of 50 μg/L (Mushtaq et al., 2018; Nickson et al., 2005). The fate and toxicity of As in different environmental matrices depend on a multifaceted series of controlling factors, including the biological processes, chemical speciation and mineralogy of the area (Bowell et al., 2014). The As compounds are widely used in the manufacturing, wood preservation, and glass production industries. In past, As an As bearing compounds were widely used for the preparation of insecticides, herbicides, and fungicides, as well as feed additives (Mandal and Suzuki, 2002). Anthropogenic sources of As include the disposal of municipal, industrial and domestic waste into the water system and coal combustion, which also releases **As** to different environmental matrices (Ali et al., 2018). There are four geological processes that naturally release As into various environmental compartments namely, reductive dissolution, sulfide oxidation, alkali desorption and geothermal activities (Brammer and Ravenscroft, 2009). In South Asian regions, reductive dissolution is the most important mechanism that releases As in groundwater (Shakoor et al., 2018). The Various mechanisms have been proposed for the release of As in groundwater, among these, the widely accepted is desorption of As from iron oxyhydroxides

☆ This paper has been recommended for acceptance by Bernd Nowack.
* Corresponding author.
E-mail address: afarooqi@qau.edu.pk (A. Farooqi).

https://doi.org/10.1016/j.envpol.2018.10.103
0269-7491/

$Fe(OH)_2$ in the sediments and as a result of microbial degradation, the ferric iron (Fe^{3+}) reduces to the soluble form, *i.e.* ferrous iron (Fe^{2+}) and As releases in groundwater (Nickson et al., 2000). The other is oxidation of As-bearing sulfide minerals (Farooqi et al., 2007b).

The change in hydrological conditions along with alterations in groundwater flow paths play a vital role in controlling arsenic mobilization in aquifers. For this purpose, isotopic compositions and comparisons between precipitation and groundwater are used to understand the recharge mechanism of groundwater, and its ultimate effect on arsenic release into aquifers (Yeh et al., 2014).

The stable isotopes of Hydrogen (δ^2H) and Oxygen ($\delta^{18}O$) are now commonly and widely used for the tracing of flow systems and the reconstruction of climate (Zhu et al., 2007). The δ^2H and $\delta^{18}O$ isotope compositions of water are also used as tracers to understand the hydrological processes of ground and surface water interactions, precipitation and basin hydrology (Gat, 1996; Mushtaq et al., 2018). A number of studies have use the stable δ^2H and $\delta^{18}O$ isotopic compositions of arsenic contaminated water as to understand groundwater recharge sources and its effect on the arsenic mobilization in groundwater (Aziz Hasan et al., 2009; Mladenov et al., 2014; Mukherjee et al., 2007; Xie et al., 2012).

Geographically, Pakistan is categorized by different land cover and altitudinal settings, including the mountains of Karakoram, Himalaya and Hindukush ranges located in the North, the Flat-lying Indus plain in the East, in West the highland Baluchistan plateau and the costal belt of Arabian sea situated in the Southern region (Fig. 1a) of the country (Eqani et al., 2016). The major land areas in Pakistan (Sindh and Punjab Provinces) are covered by the Flat-lying Indus Plain, which contains sediments that are mainly of alluvial and deltaic origin and predominantly Quaternary (Pleistocene) in age; the thicknesses of these sediments range from several meters to hundred meters in various parts of the country (Mushtaq et al., 2018). The aquifers in these sedimentary areas are contaminated with high **As** concentrations (Shakoor et al., 2018). The recent deposits of alluvial and deltaic sediments, especially those in Pakistan (Sindh and Punjab regions), India (West Bengal regions) and Bangladesh, have very similar geochemical compositions (Ali et al., 2018). It has thus been predicted that the processes of **As** mobilization in these areas are almost the same. In Pakistan, oxidizing conditions and the presence of unconfined aquifers cause lower concentrations of **As** in groundwater as compared with those in India and Bangladesh (Ali et al., 2018). Previous studies have shown that several areas of Sindh and Punjab provinces were highly affected by contamination in groundwater derived from both anthropogenic and natural sources of As (Farooqi et al., 2007a; Nickson et al., 2005). According to (Rahman et al., 1997), the maximum As concentration in the groundwater of Karachi of 80 μg/L exceeded the allowable limits (10 & 50 μg/L) of the WHO and the Pakistan Standards and Quality Control Authority (PSQCA). Approximately 13 **to** 16% of the population of Sindh Province and 23% of the population of Punjab Province are severely at risk due to the consumption of **As-**contaminated groundwater. A study was conducted by (Farooqi et al., 2007a) in Kalalanwala, Kasur Lahore Punjab, reported a maximum concentration of As in groundwater of 2400 μg/L. While, Multan and Muzaffargarh groundwater the maximum As concentration 400 and 1000 μg/L respectively was reported by (Nickson et al., 2005). Similarly, in Sindh, the highest level of As 2580 μg/L has been reported in Tharparkar (Brahman et al., 2013). Though (Arain et al., 2009), reported that the maximum concentration of As in groundwater in the adjacent areas of the Manchar lakes ranged from 23.3 to 96.3 μg/L. According to the published literature, in other various parts of Pakistan, such as Jamshoro, Khairpur, Nagar Parker, Rahim Yar Khan, Mailisi, Hasilpur and Multan adjacent regions, the concentrations of As are as high as 100 μg/L (Baig et al., 2011; Haque et al., 2008; Rafique et al., 2009; Rasool et al., 2016; Rabbani et al., 2017; Shakoor et al., 2018; Tabassum et al., 2018). After two decades of the first incidence of As pollution lot of studies have been done on water characteristics in relation to As however, up till now there has been no work to evaluate the effect of return irrigation flow in an extensive irrigated areas of Indus basin where groundwater is extensively used for the irrigation purposes.

The main objectives of this study is 1) to understand the effects of groundwater recharge on the mobilization of As and its concentration level in groundwater by using geochemical analysis, 2) to understand vertical mixing by isotopes of hydrogen and oxygen and its role in controlling arsenic concentrations, 3) effect of return irrigation on the mobilization of As and the mineral phases associated with high As in groundwater. The significance of this study is to help with the future development of diverse As mitigation measures at both regional and national levels and to better adopt the irrigation practices to control the release of As in the groundwater.

2. Materials and methods

2.1. Study area

Larkana district is located along the Indus River and contains five Tehsils, Dokri, Warah, Miro Khan, Larkana, and Ratodero (Fig. 1) with a total area of 7423 km^2. Larkana is the fourth-largest city in Sindh Province. According to the 2017 census of Pakistan, the overall population of the district is 1.5 million; about 30% of this population is urban and the population growth rate is 3.24% (CENSUS, 2017). The soils of the area are classified as non-saline to saline (Wagan et al., 2002). The groundwater is the primary source of drinking water. The groundwater in this district is under constant threat of contamination due to highly saline soils and return irrigation flow where groundwater is used for the irrigation purpose along with the canal irrigation and poor drainage that has increased the salinity in the study area (Qureshi et al., 2008).

2.2. Climate

In the study area, the climate is semi-arid to arid and hot (Rehman et al., 1998). In summer, it is very hot, and the maximum temperature reaches up to 53 °C; in winter, the temperature drops down up to 12 °C (Chandio and Anwar, 2009). The average rainfall in Larkana district is approximately 100–125 mm/year. Sometimes, monsoons cause heavy rains that bring floods to nearby areas (Chandio and Anwar, 2009).

2.3. Sampling and analytical methods

In summer July 2016 a total of 58 groundwater samples were collected from pre-existing wells (hand pumps and boreholes) located at various depths ranging from 10 to 24 m from the four selected sites of *Larkana* (L), *Naudero* (ND), *Ghari Khuda Buksh* (GK) and *Dokri* (D) for isotopic and hydro-chemical analysis. Additionally, 4 canal water samples were also collected from a rice canal following the protocol defined by (Grynkiewicz et al., 2003), and 4 rainwater samples were also collected for hydro-chemical analysis. Rainwater was collected by placing rainwater gauges at different locations in the study area to obtain representative precipitation samples. The gauges were manually operated; they were left open during rainy periods and covered with a lid during non-rainy days to reduced evaporation. The locations of sampling sites are shown in (Fig. 1). The pH and Electrical Conductivity (EC μS/cm) were measured in the field by using a pH/EC meter (HANNA instrum

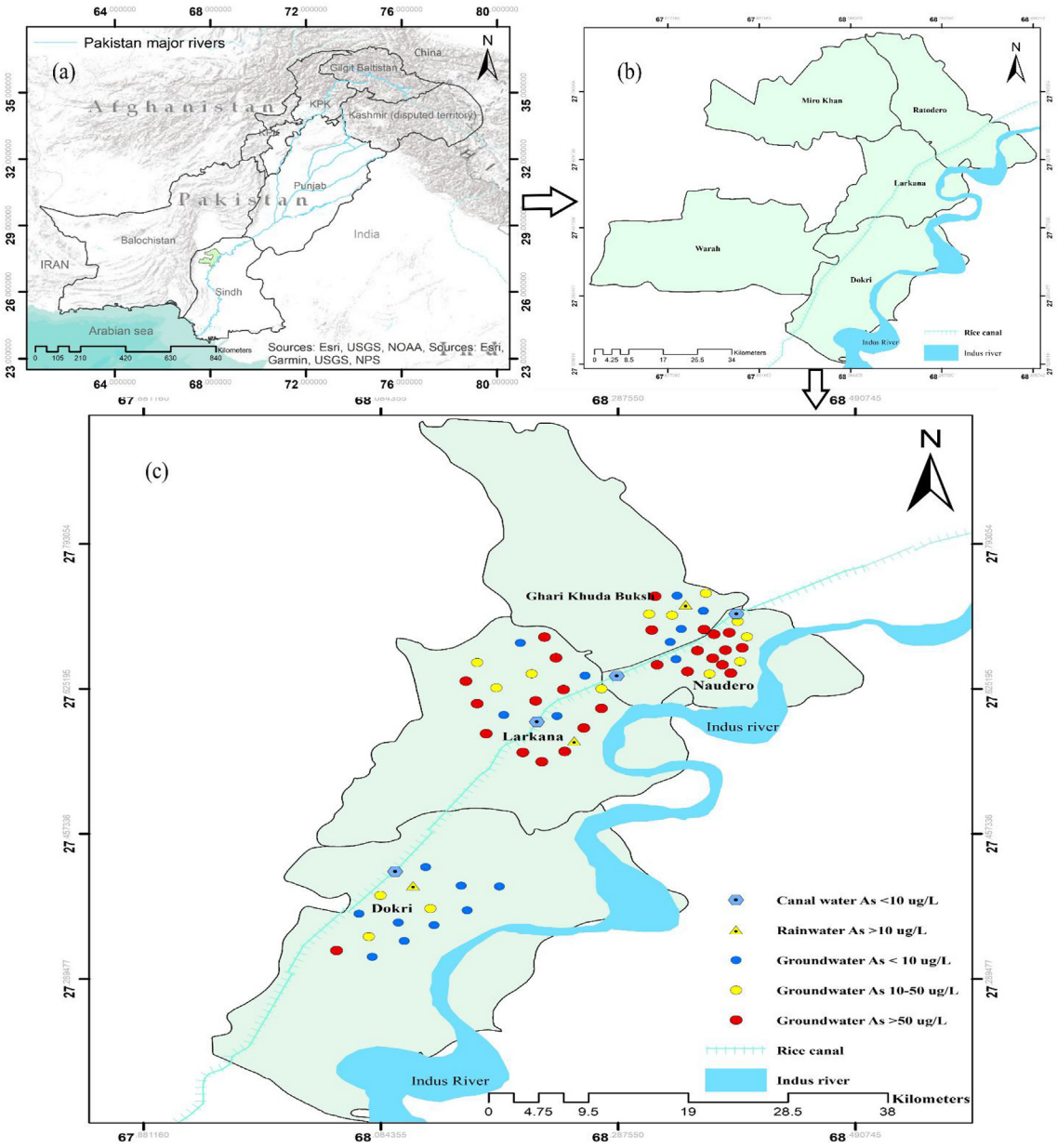

Fig. 1. Sampling location map with spatial distributions of As, groundwater, rainwater and canal water.

ents). Oxidation-Reduction Potential (ORP) was measured using a meter (pH-7110-Inolab-WTW Intertek); these data were later corrected with respect to standards. Eh calculations were performed using the following equation (Nordstrom and Wilde, 2005).

$$\text{Eh (sample) (V)} = \text{E obs} + \text{E ref} \quad (1)$$

where E*obs* is the observed ORP values measured in the field, and E*ref* is the Ag/AgCl reference electrode (236 mV) containing 1 M KCl solution electrodes; the pH/EC and ORP instruments are calibrated daily before analysis. The contents of total dissolved solids (TDS) were also measured indirectly by using electrical conductivity values and using the conversion factor specified by (Moharir et al., 2002).

$$\text{TDS (mg/L)} = \text{EC (}\mu\text{S/cm)} * 0.67 \quad (2)$$

All samples were collected after purging for 3–5 min, filtered (0.4 μm) at site and stored in 120 ml plastic (propylene) bottles by following the standard sampling protocols and methods defined by (APH, 2005). All samples were collected in duplicate for major anion and cation analysis. Samples collected for major anion (SO_4^{2-}, PO_4^{3-}, NO_3^-, CO_3^{2-}, HCO_3^-, Cl^-) analysis were filtered and preserved, while samples collected for major cation (Na^+, K^+, Mg^{2+}, Ca^{2+}) analysis were acidified with hydrochloric acid (HCl) to pH values of <2 before preservation. For isotope $\delta^{18}O$ and δ^2H analysis, samples were collected in glass bottles that were filled up to the mouth and tightly capped to reduce the effect of water evaporation for their analysis.

To maintain and assure the quality and integrity of samples, important quality control measures were taken from sample collection to sample analysis. Replicate of samples ensured that the cross-contamination was minimized during sampling and instrument was calibrated prior to analyses. In addition, all chemical reagents used were checked and made sure to be of analytical grade

to minimize the chance of random errors. All samples were tightly capped and store at 4 °C and were transported to the Pakistan Institute of Nuclear Science and Technology (PINSTECH) at the Isotope Application Division (IAD) laboratory for stable isotope $\delta^{18}O$ and $\delta^{2}H$ and chemical analysis. The concentrations of PO_4^{-3} and SO_4^{-2} were measured using UV–Visible spectrophotometry (APHA, 2005) while the concentration of NO_3^- in groundwater was determined potentiometrically by using an Ion Selective Electrode (ISE) (Oakton Ion 5, acron series). The ISE was calibrated against a set of standards with known NO_3^- concentrations, and a calibration curve was made. The NO_3^- contents in water samples were determined by comparing their potential difference values with standard curve (APHA, 2005). Alkalinity was measured using the acid-base titration method to determine carbonate and bicarbonate contents; chloride contents were determined using the argentometric titration method (Kelly et al., 2005). The cation and trace metal contents in samples (Na^+, K^+, Mg^{2+}, Ca^{2+}, and Mn) were analyzed by Sequential Atomic Absorption Spectroscopy (GTA110 Varian) (Kelly et al., 2005). The total **As** contents in samples were analyzed using a continuous flow hydride generation atomic flame Spectrophotometer (AI-3200 series, Aurora Instruments). The $\delta^{2}H$ and $\delta^{18}O$ were done by using delta-plus Isotopic Ratio Mass Spectrophotometer (IRMS) with the continuous flow – Inlet technique. The analytical precision of $\delta^{2}H$ and $\delta^{18}O$ was ±1.2‰ and ±0.05‰, respectively (Clark and Fritz, 1997).

2.4. Statistical and geological analysis

Multivariate statistical analysis was performed using the computer-based software programs Statistica 7.0 and XLSTAT. The spatial distribution and investigation of the ionic ratios Na^+/Cl^-, Mg^{2+}/Ca^{2+} and Cl^-/HCO_3^- were calculated by following equations;

$$\text{Cation or anion mmol/L} = \text{Cation or anion mg/L/ Molecular weight} \quad (3)$$

$$\text{Ionic ratios} = \text{Cation or anion (mmol/L)/Cation or anion (mmol/L)} \quad (4)$$

The distribution maps, were made using Geographical Information System (GIS) techniques and by applying the ordinary kriging method. The kriging method is one of the best interpolation techniques in (ArcGIS 10.2). Applying basic geo-statistical tools for modeling spatial autocorrelation regionalizes semi-variogram variables, which represent the average measure of the degree of dissimilarity between an unsampled value and the nearest data values (Deutsch and Journel, 1998).

2.5. Geochemical modeling/saturation indices (SI)

Saturation indices (SI = log [IAP/KT]) were calculated for the present data to predict themineralogy in the area. IAP is the Ion Activity Product while KT is the equilibrium constant of a specific mineral phase at room temperature. SI values were calculated using the computer-based geochemical program PHREEQC (Interactive 2.11) and the WATEQF database.

3. Results and discussions

3.1. Aqueous hydro-geochemistry

The statistical summary of chemical and isotopic composition of groundwater is given in Table 1. Pearson correlation and summary of canal and rainwater is provided in the form of supplementary information (Tables S1 and S2).

The groundwater samples all four sites were neutral to alkaline in nature with pH ranging from 6.8 to 8.1 (average = 7.4). *Naudero* and Larkana groundwater samples having higher pH values as compare with *Ghri Khuda Buksh* and *Dokri*. All groundwater samples have very high spatial variation within EC (μS/cm) and total dissolved solids (TDS mg/L) ranging between 600 and 5300 μS/cm (mean = 1293). Highest EC values were reported in Dokri 800–5300 (mean = 2644), 84.6% Samples exceed WHO permissible limit.

Major cations composition in all groundwater samples of current study follow following order based on their abundance values $Na^+ + K^+ > Ca^{2+} > Mg^{2+}$. Sodium ($Na^+$) is major Cation in Dokri and Larkana with 92%, 50%, exceeding the WHO limit of 200 mg/L. While in Nudero and Ghari Khud Buksh in some samples Ca^{2+} and Mg^{2+} exceeded over the Na^+. The following order was observed for Na^+ concentration in groundwater on the basis of their abundance *Dokri* > *larkana* > *Naudero* > *Ghari Khuda Buksh*. While major anions composition in all groundwater samples follow the following order on the basis of their high concentration $Cl^- > SO_4^{2-} > NO_3^-$, with the order Dokri > Naudero > Larkana > Ghari Khudabuksh respectively.

The highest Cl^- concentration in groundwater of present study was measured at Dokri which ranged from 309 to 5715 (mean = 1757 mg/L) 100% samples exceeded exceed WHO permissible 250 (mg/L), Naudero groundwater samples contain 119–532 (mean = 322 mg/L) with 70% samples exceeded, Larkana chloride ranged from 111 to 425 (mean = 274 mg/L) with 70% of samples exceeded and in Ghari Khuda Buksh chloride concentration were measured ranged from 90 to 496 (mean = 237 mg/L) where 20% of the groundwater samples exceed WHO permissible limit of 250 (mg/L).

The chemical compositions of groundwater was identified by plotting a Figure as proposed by (Chadha and Ray, 1999) (Fig. 2). The Figure showed 92% samples from Dokri, 11 73% from Naudero, 50% of Larkana, and 40% of Ghari Khuda Buksh were Na^+-Cl^- type with the high EC (μS/cm). While (40%) of Ghari Khuda Buksh, 25% of Larkana, 20% of Naudero were Ca^{2+}-Mg^{2+}-Cl^- type. Only 4 samples of Larkana (20%), 2 samples of Ghari Khuda Buksh (20%) of water is Ca^{2+}- HCO_3^- type (Fig. 2). The hydrogeochemical evolution of groundwater of an area is mostly controlled by various cationic and anionic reactions occurring in an aquifer system, the residence time of groundwater, rock-water interaction and chemical compositions of recharging water (Mukherjee et al., 2007). For recognition of groundwater chemistry, sources of solutes and natural process that control groundwater chemistry in 1970 Gibb's proposed a plot between total dissolved solids (TDS) versus $Na^+ + K^+/Na^+ + Ca^{+2} + K^+$ for cations and TDS versus $Cl^-/Cl^- + HCO_3^-$ for anion. The plot specifies in four fields, 1st evaporation dominance field, 2nd evaporation – precipitation dominance field and 3rd rock dominance field (Gibbs, 1970). In (Figure S 1) 100% groundwater samples of Larkana, Naudero and Ghari Khuda Buksh fall in rock dominance and 54% of samples of Dokri also fall in rock dominance field while 46% samples fall in evaporation-precipitation dominance field. The results show that the rock weathering process controlling groundwater chemistry. The highest concentration of major cations Na^+, $Mg^{+2}$and Ca^{+2} may be due to the weathering of minerals or rock solution mixing in the aquifer system (Malana and Khosa, 2011). The most dominant Na^+-Cl^- type of groundwater in all sampling sites (Fig. S1) due to the high rates of evaporation that causes high ionic strength of groundwater or groundwater could be the result of mixing of fresh water with saline water (Ekwere et al., 2012). The hydrogeochemical facies and Gibbs plots confirm that alkali Na^+ exceeds over alkaline Ca^{+2}-Mg^{+2}-Cl^- and HCO_3^- suggesting saline water in Dokri and Larkana (Mukherjee et al., 2008).

Table 1
Descriptive statistics of physicochemical parameters of groundwater samples with saturation indices (SI) of current study sampling site wise.

Parameters	WHO	Larkana (N = 20)				Naudero (N = 15)				Ghari Khuda Buksh (N = 10)				Dokri (N = 13)			
		Min	Max	Mean	SD	Min	Max	Mean	SD	Min	Max	Mean	SD	Min	Max	Mean	SD
Well Depth (m)	–	10	24	16	4	10	20	14	4	11	21	16	4	14	24	20	2.5
pH	6.5–9.2	6.9	8.1	7.5	0.4	7.1	8.1	7.6	0.3	6.9	7.8	7.4	0.3	6.8	7.6	7.1	0.23
Eh (mV)	–	−225	−60	−150	42	−155	−110	−131	14	−155	−75	−118	24	−175	−75	−120	27
EC (μS/cm)	1500	600	1310	909	202	710	1200	887	162	710	1430	912	219	800	5300	2644	1755
TDS (mg/L)	600–1000	360	786	545	121	426	720	532	97	426	858	547	131	480	3180	1586	1053
HCO_3^-(mg/L)	–	260	650	359	84	220	440	325	56	220	350	272	36	280	800	432	164
T.H eqv. $CaCO_3$(mg/L)		178	375	302	48	264	541	352	83	229	511	313	85	206	2218	781	661
Cl^-(mg/L)	250	111	425	274	88	119	532	322	109	90	496	237	134	309	5715	1757	1878
SO_4^{2-}(mg/L)	250	1	39	17	11	13	49	28	10	6	35	17	11	25	640	175	214
NO_3^-(mg/L)	50	0	7.8	2.7	2.1	0	5.2	1.3	1.9	0	3.8	1.2	1.6	0	4.5	1.9	1.8
PO_4^{3-}(mg/L)	0.1	Bdl	Bdl	Bdl	Bdl	Bdl	Bdl	Bdl	Bdl	Bdl	Bdl	Bdl	Bdl	Bdl	Bdl	Bdl	Bdl
Na^+(mg/L)	200	50	341	191	82	63	351	188	68	51	309	138	80	145	2965	1051	1042
K^+(mg/L)	12	4	13	9	2	7	27	11	7	6	13	9	3	6	80	28	29
Ca^{2+}(mg/L)	100	33	88	57	15	56	104	78	14	43	91	70	16	29	150	91	35
Mg^{2+}(mg/L)	50	23	52	39	9	25	69	38	13	24	71	34	15	32	449	135	143
Fe (mg/L)	0.3	Bdl	Bdl	Bdl	Bdl	Bdl	Bdl	Bdl	Bdl	Bdl	Bdl	Bdl	Bdl	Bdl	Bdl	Bdl	Bdl
Mn (μg/L)	500	100	690	340	200	100	760	380	210	0.0	500	200	200	0.0	410	80	110
As (μg/L)	10	5	279	72	76	6	318	104	92	0	126	39	45	0	53	10	14
δ^2H (‰)	–	−69.08	−58.63	−65.86	2.91	−69.16	−62.04	−66.93	1.75	−68.16	−64.48	−66.17	1.04	−70.78	−56.01	−66.47	3.90
$\delta^{18}O$ (‰)		−10.92	−7.92	−10.11	0.69	−10.16	−8.68	−9.77	0.36	−10.12	−9.35	−9.77	0.25	−10.57	−7.35	−9.51	0.85
SI Calcite	–	−0.4	0.6	0.2	0.3	−0.2	0.3	0.1	0.2	−0.2	0.4	0.1	0.2	−0.3	0.8	0.1	0.3
SI Dolomite	–	−0.7	1.4	0.5	0.5	−0.4	0.6	0.2	0.3	−0.4	0.6	0.2	0.3	−0.2	1.8	0.7	0.7
SI Gypsum	–	−3.9	−2.0	−2.7	0.4	−2.6	−2.0	−2.3	0.1	−2.9	−2.2	−2.6	0.3	−2.7	−1.4	−2.0	0.4
SI Pyrolusite	–	−24.5	−18.7	−22.1	1.7	−23.2	−21.2	−22.3	0.6	−23.6	−20.3	−22.5	1.0	−22.8	−22.1	−22.3	0.3
SI Rhodochrosite	–	−0.3	0.5	0.1	0.2	−0.3	0.3	0.0	0.2	−1.3	0.1	−0.5	0.7	−0.1	0.3	0.0	0.2

N= Number of samples, Bdl = Below detection limit, ‰ Per mill, Detection limits for As = 2 μg/L, PO_4^{3-} = 0.01 mg/L, Fe = 0.01 mg/L, Mn = 0.025 mg/L, VSMOW- Vienna Standard for Mean Ocean Water.

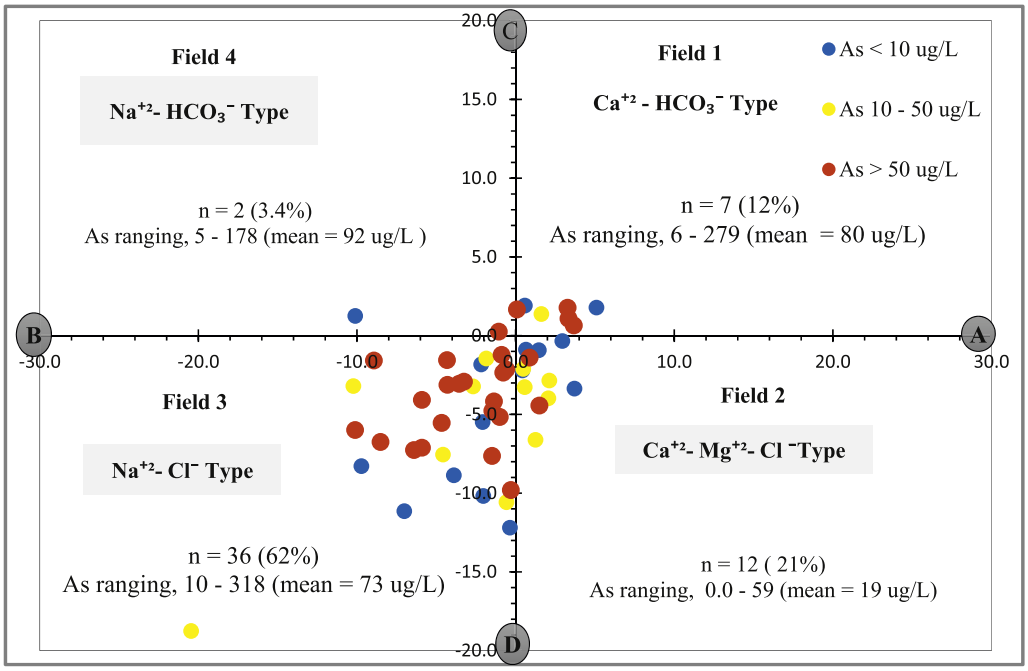

Fig. 2. The chemistry of groundwater in the area with As concentrations.

3.2. Spatial distribution of EC and ionic ratios in groundwater

Fig. 3a shows that EC (μS/cm) gradually increases from the northwest to southwest (i.e., from Naudero towards Dokri); the highest electrical conductivity is measured in Dokri, this trend of EC shows that there may be evaporation factor involved which can increase the EC values (Sheikhy Narany et al., 2014). The water type in this area is sodium chloride type as shown in Fig. 2. The soils of this area are highly saline and salinity increases because of the high evaporation (Wagan et al., 2002).

The molar ratios of cations and anions can determine the source of these ions in water. In groundwater, Ca^{2+}/Mg^{2+} molar ratio of equal to one or <1 indicates the dissolution of dolomite rocks (Mayo and Loucks, 1995). A Ca^{2+}/Mg^{2+} ratio of >2 reflects the dissolution of silicate minerals (Katz et al., 1997). In 50% of all groundwater samples, the Ca^{2+}/Mg^{2+} ratios ranged from 1 to 2, thus

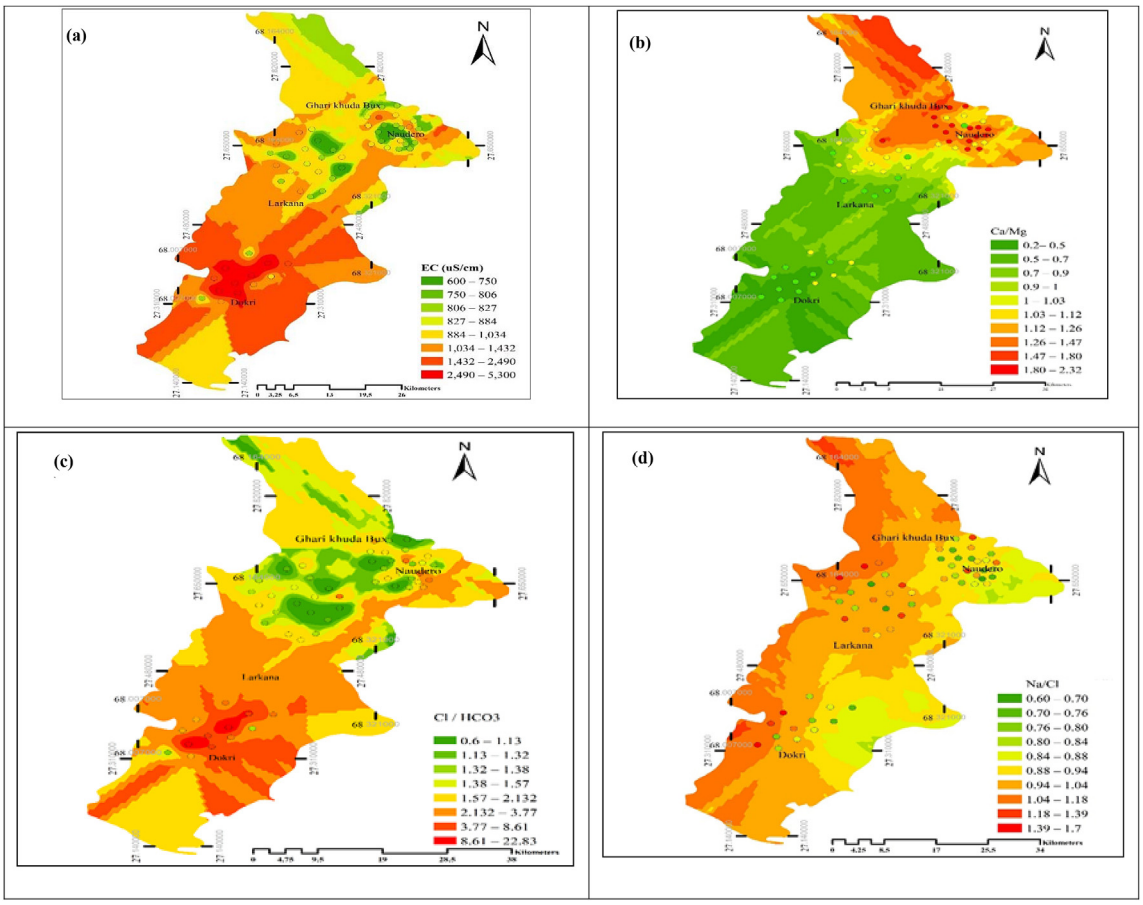

Fig. 3. Spatial distribution (Kriging) of (a) EC (μS/cm) (b) Ca^{2+}/Mg^{2+} (c), Cl^{-}/HCO_3^{-}, (d) Na^{+}/Cl^{-} respectively of study area groundwater.

indicating the dissolution of calcite minerals; 17% of groundwater samples record ratios of <1, thus reflecting the dissolution of dolomite minerals; and 33% of samples record ratios of >2, thus reflecting the dissolution of silicate minerals (Fig. 3b).

The spatial distribution of Cl^{-}/HCO_3^{-} molar ratios (Fig. 3c) indicates that the *Larkana* and *Ghari Khuda Buksh* samples are characterized by natural water, while high salinization influences *Dokri*, near the southwest side of the study area, which is likely exaggerated by saline water. A Na^{+}/Cl^{-} ratio of equal to one indicates that halite dissolution may be responsible for the Na^{+} concentrations in groundwater; in (Fig. 3d), the spatial distribution map of Na^{+}/Cl^{-} reveals that in most of the study areas of *Larkana* and *Dokri*, these ratios are higher than 1.5, which indicates that the source of Na^{+} is silicate weathering. Groundwater salinity also may be due to the formation of a salt layer through the process of leaching from the soil surface during high evaporation (Wagan et al., 2002).

3.3. Arsenic distribution and its behavior with manganese and other redox parameters

The As concentration in all groundwater samples ranged from below detection limit (Bdl) 2–318 μg/L (mean = 61 μg/L). Over all 67% samples exceeded the WHO permissible limit of 10 μg/L. Highest concentration is observed in Naudero with 86% samples exceeding the WHO permissible limit. Whereas, in *Larkana*, *Ghari Khuda Buksh* and *Dokri* the samples exceeding are 75, 60 and 31% respectively, pH, Eh, Mn and Fe are the main redox parameters which control the release of As in groundwater. In the present study Fe concentrations were within the permissible limits of 0.3 mg/L. Whereas, the highest Mn concentration was measured in Naudero ranged from 100 to 760 (mean = 380 μg/L) with 40% groundwater samples exceeded the WHO permissible limit of 500 (μg/L), while the Larkana and Ghari Khuda Buksh the Mn concentration ranged from 100 to 690 (mean = 340 μg/L) and 0 to 500 (mean = 200 μg/L) with 20% and 10% samples exceeding the WHO permissible limit. While the lowest Mn concentration was measured in Dokri groundwater samples ranged from of 0.0–410 (mean = 80 μg/L) all of the samples within WHO permissible limit (Table 1).

Fig. 4a and b shows the correlation of As, Mn, pH and Eh. It is clear from Fig. 4a that high As is present at relatively lower pH and negative Eh values The similar trends of groundwater As and Mn and pH values were observed at all sites as shown in (Fig. 4b) with the increase in Mn concentrations the As concentrations increases with low negative Eh and low pH. In *Naudero*, elevated groundwater As concentration were observed at neutral pH (mean = 7.2), negative Eh (mean = −131 mV) and high levels of HCO_3^{-} (mean = 325 mg/L) and Mn (mean = 380 μg/L) suggesting reducing nature of groundwater. This fact is further supported by the presence of low levels of SO_4^{-2} (mean = 28 mg/L) and NO_3^{-} (mean = 1 mg/L). In (Fig. 5a) slight positive correlation were observed between NO_3^{-} and As ($r^2 = 0.3$), while no such relation was observed between NO_3^{-} and Mn (Fig. 5b) in all water samples. In *Larkana*, the concentrations of As, Mn and sulphates (SO_4^{2-}) were generally lower than that observed in *Naudero*. A negative correlation of **As** with pH ($r^2 = -0.34$) and Eh ($r^2 = -0.6$) was detected indicating a generally decreasing trend of **As** values at higher pH and positive Eh values in all sites (Fig. 5c and d). The similar trend was observed for Mn with pH and Eh (Fig. 5 e and f). A positive

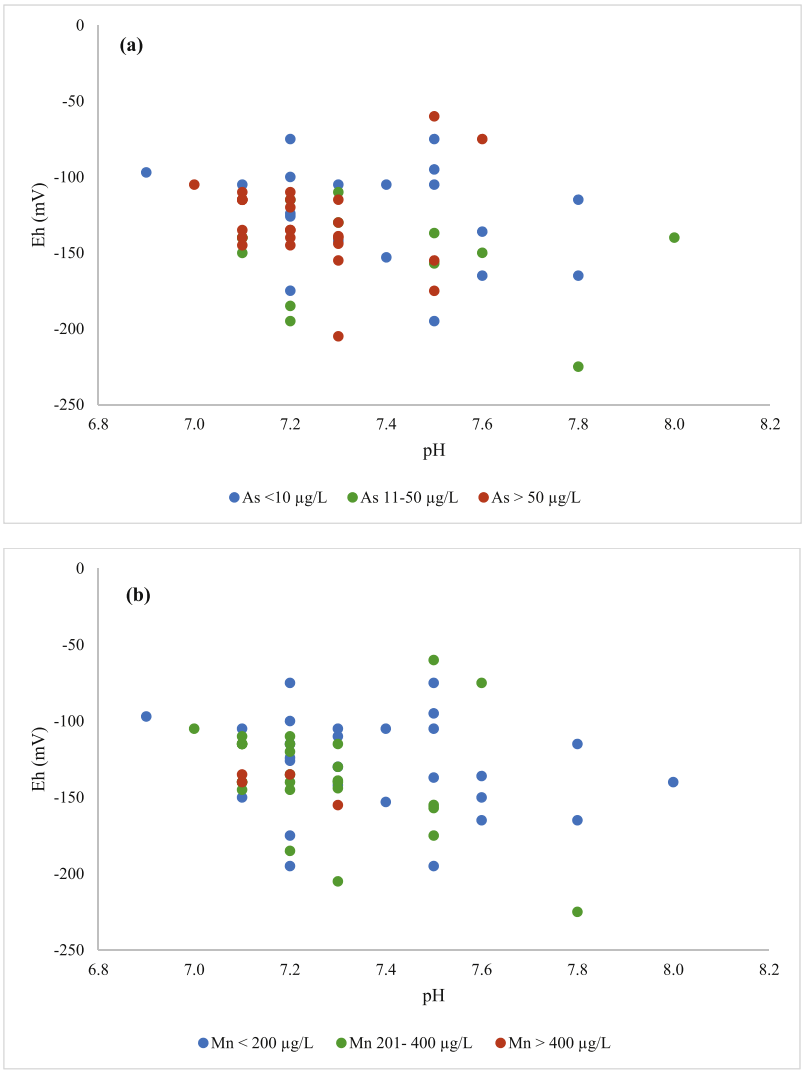

Fig. 4. The behavior of As and Mn as a function of Eh-pH diagram. Higher concentrations of As and Mn were observed at neutral pH values (7–7.5) and at reducing conditions (Eh < -100 mV).

correlation between Mn and As was observed as shown in (Fig. 5 g, Table S2). In all above three sites As release is seemed to be trigged by reductive dissolution of As from Mn-oxide surfaces. Such type of As release mechanism has been reported from vast areas of South and South-East Asia (McArthur et al., 2008). Furthermore, the presence of elevated As and Mn (Fig. 5h and i) levels at shallower depths (11–18 m) also indicate poor drainage capacity of aquifers enhances the reducing nature of groundwater (Buschmann et al., 2007).

In *Dokri*, overall low groundwater As concentrations were observed with only 31% of samples having As levels above WHO limit. High values of pH (7.8) and SO_4^{2-} (640 mg/L) along with very low nitrate (NO_3^-) and moderate Eh (−75 mV) values indicate conditions not completely reducing enough for complete reduction of SO_4^{2-} to occur (Pi et al., 2018). This partial anoxic condition of groundwater at this site might be one of the possible reasons behind the existence of low levels of As in the study area. Moreover, the spatial distribution of As behavior shows a decreasing trend in its concentrations as we move down along the Indus river flow as shown earlier in (Fig. 1). The reason for these low concentrations maybe because At lower basin of Indus river with low river flow, deep alluvial deposits and partial anoxic conditions may control release of As in shallow aquifer (Naseem and McArthur, 2018).

3.4. Mineral phases, sources of manganese and its role in arsenic solubility

Various igneous and metamorphic rocks are significant sources of Mn, which is released as divalent manganese (Mn^{2+}). Once Mn^{+2} is released in groundwater through weathering it precipitates as Mn^{4+} oxide when it exposed to the atmosphere. In contrast, dissolved Mn is always present in the 2^+ oxidation state in the natural water system (Hem, 1972). The saturation indices (SI) of rhodochrosite ($MnCO_3$) range from −1.29 to 0.46. The ranges observed at each site are listed in (Table 1). The solubility of $MnCO_3$ control the Mn concentrations in the groundwater of the present study area. The slight positive correlation between As and Mn may contribute to the release of As into the groundwater system (Vega et al., 2017; Woo and Choi, 2001). The overall solubility of $MnCO_3$ likely control the concentration of Mn in the groundwater of the present study

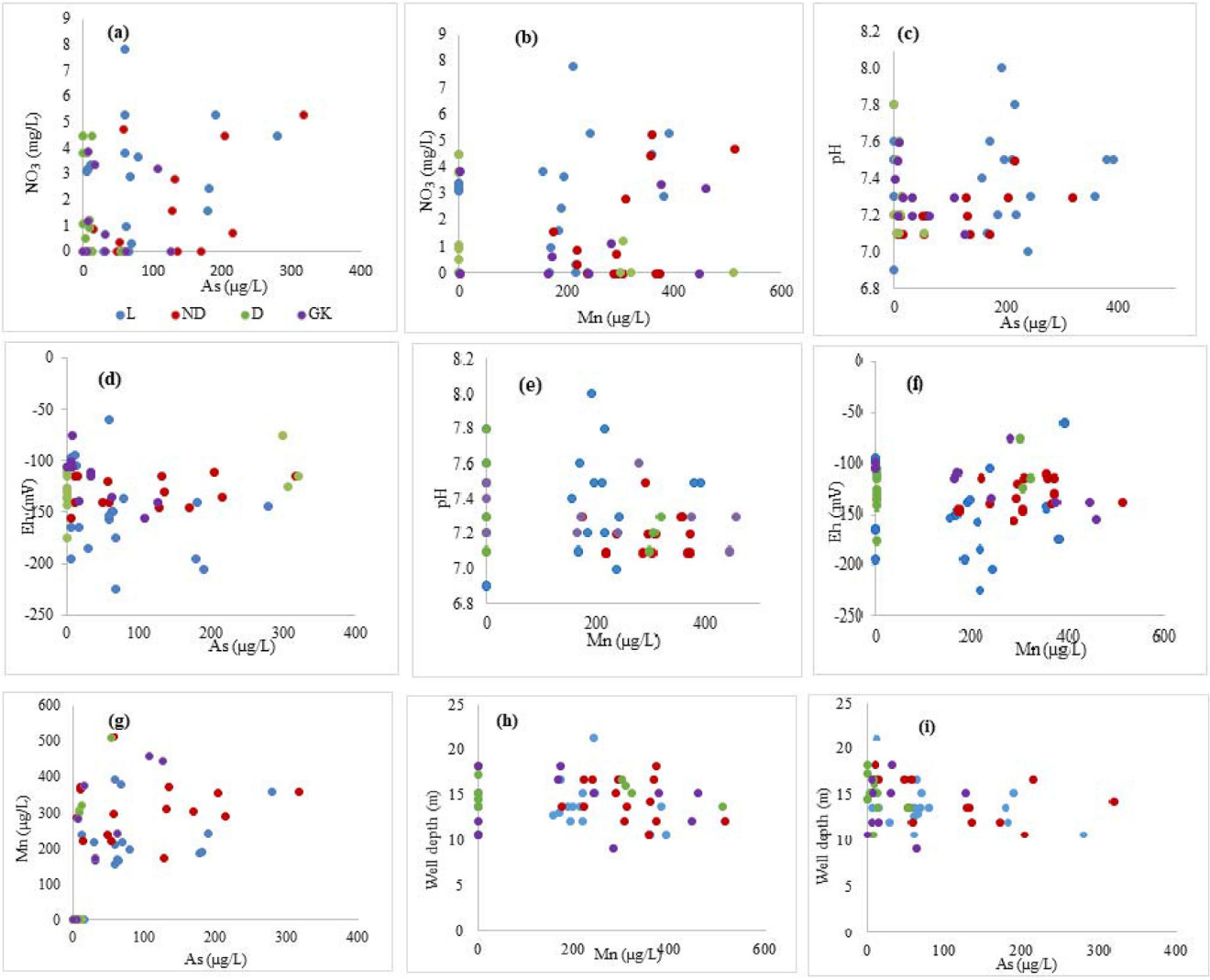

Fig. 5. As and Mn scatter plots (a) NO_3^- with As (b) NO_3^- with Mn (c) pH with As, (d)Eh with As, (e) pH with Mn (f) Eh with Mn, (g)As variability in groundwater as function of Mn, (h) Well depth with Mn and (i) Well depth with As is shown.

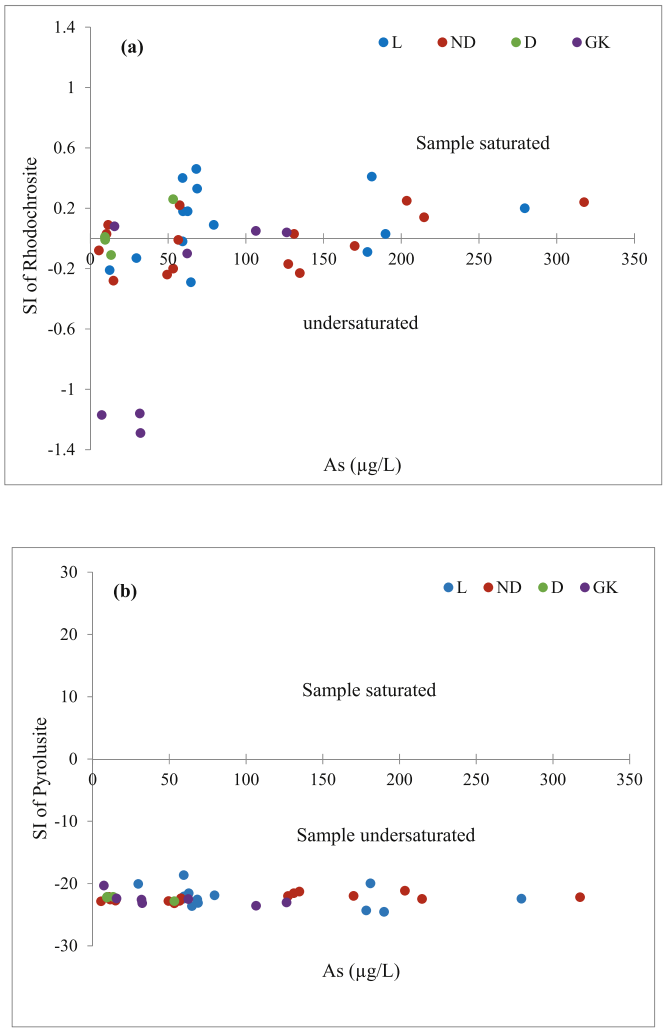

Fig. 6. The sitewise relation in between different chemical components of groundwater (a) samples saturation indices (SI) of rhodochrosite with As (b) SI of pyrolusite with As.

area. The results of the present study support the universal concept that As occurs in very moderately and typically Mn-rich groundwater; thus, anaerobic heterotrophic bacteria may be responsible for the reductive dissolution of Mn minerals and the release of As into groundwater (Routh and Saraswathy, 2004). The positive correlation As with Mn suggests (Table S2) the As might be adsorbed onto Mn-hydroxide and As released in groundwater through low redox conditions (Nath et al., 2008a; Nath et al., 2008b). It has been extensively known that Mn dissolved in groundwater by reductive dissolution process from Mn-hydroxide. Through dissolution mechanism the free As and Mn releases into aquifers (Choudhury et al., 2015; Saunders et al., 2005; Zheng et al., 2004; Zhu et al., 2015). The samples above 0 the positive values consider as saturated and below 0 with negative values indicate undersaturated. The $MnCO_3$ versus As (Fig. 6a), suggest 45%, 40% and 30% of samples from *Larkana*, *Naudero* and *Ghari Khuda Buksh* respectively saturated with respect to $MnCO_3$. The SI values (Fig. 6b) of Pyrolusite (MnO_2) versus As indicate that all samples are undersaturated; in the future, further dissolution may cause increased As concentrations in groundwater.

3.5. Vertical mixing and irrigation return is probably the main process controlling the enrichment of high arsenic in groundwater

The isotopic (δ^2H and $\delta^{18}O$) composition of the ground, rain and river water samples are given in Table 1. For present study, δ^2H and $\delta^{18}O$ relative to VSMOW showed variation between −70.78 and −56.01‰ and −10.92 and −7.35‰ respectively. Based on isotope composition of δ^2H and $\delta^{18}O$ in rainwater, the equation of the local meteoric water line is given as follows:

$$\delta^2H = 7.4581^* \delta^{18}O + 12.044 \quad (5)$$

All the groundwater samples in present study fall on the lower end of the GMWL indicating meteoric origin of recharge. The shift of samples away from LMWL indicate mixing of vertical recharged water (precipitation and irrigation water) with evaporated pore water before infiltration (Clark and Fritz, 1997). The slope of the resulting evaporation line is 3.2 which is typical for recharging water which had undergone evaporation through soil-water infiltration. Few of the samples for groundwater also had similar isotopic composition for δ^2H and $\delta^{18}O$ as that of canal water (Fig. 7a and b) indicating canal water being another source of recharge of aquifer.

The presence of saline soil and intensive extraction of groundwater for irrigation purposes also make irrigation return water and salt flushing another source of groundwater recharge. From the plot of $\delta^{18}O$ against Cl- (Fig. 8a), it can be seen an increase in Cl-concentration causes little to moderate variation in $\delta^{18}O$. The increase in Cl-concentrations could be attributed to vertical infiltration of irrigation return water carrying significant amounts of salts from land surface. While the plot between $\delta^{18}O$ against As (Fig. 8b) shows two distinct trends. All the high As groundwater samples fall close to the low evaporation but high leaching line while all low As samples fell close to evaporation line suggesting vertically recharged water might be playing a role in As mobilization in unsaturated zone. During infiltration, irrigation return, and salt wash out gradually occupy the pore spaces of soil causing a shift from oxic to slightly anoxic conditions. Under such situations, the environment become favorable for arsenic release from sediments to aquifer (Huq et al., 2018; Xiao et al., 2018).

4. Conclusion

The groundwater in the area is sodium chloride dominated with arsenic >300 µg/L. The saturation indices of rhodochrosite ($MnCO_3$) indicated a saturated state and may control the Mn concentrations in the groundwater of the present study area, and the positive correlation between As and Mn may contribute to the release of As into the groundwater system. All of the groundwater samples in the present study fall on the lower end of the GMWL, indicating the recharge source of groundwater from highly saline water. The isotopic composition of groundwater with increasing $\delta^{18}O$ values with increase of Cl^- concentration in the study area groundwater discharge from the basin. The high Cl^- concentration and enriched $\delta^{18}O$ composition could be due to the evaporation, halite dissolution is the main important source of Cl^- along with evaporation. The groundwater samples shifted away from the local meteoric water line, representing the mixing of vertical recharge with evaporated pore water. The site wise distribution of $\delta^{18}O$ values in the As contaminated water samples ranging from 2 to 318 µg/L, suggest vertical mixing water is a significant contributor to the As mobilization in mostly Larkana and Naudero groundwater, which contain higher As contents than the groundwater in Ghari Khuda Buksh and

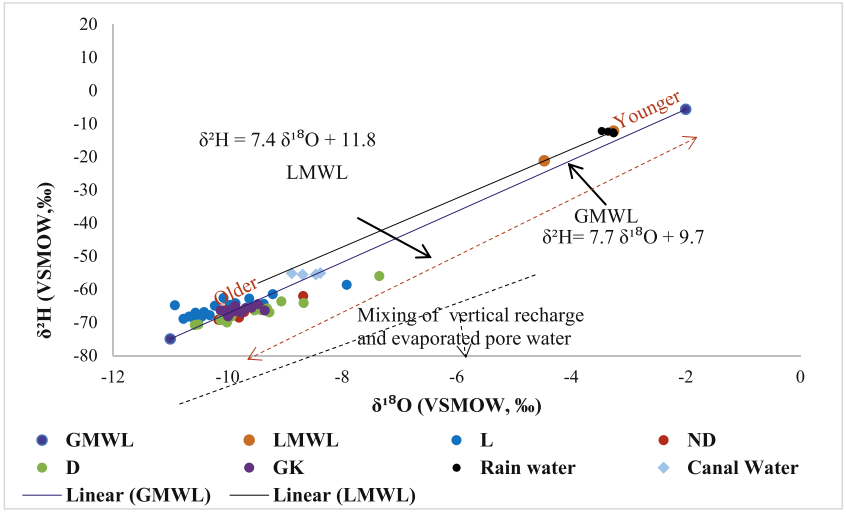

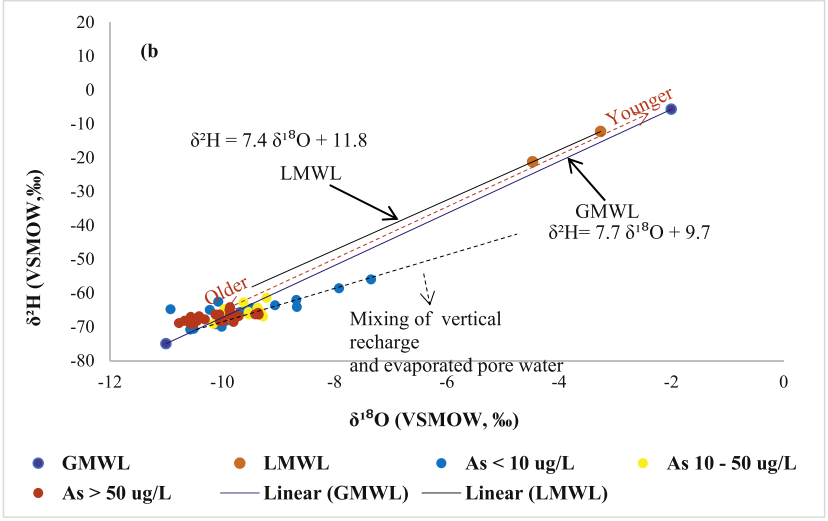

Fig. 7. (a) Isotopic composition (δ^2H and $\delta^{18}O$) of ground and canal water for the present study area while (b) shows isotopic geochemistry of low (<10 μg/L) and high (>10 μg/L) arsenic groundwater in relation to GMWL and LMWL modified after Ekwere et al. (2012).

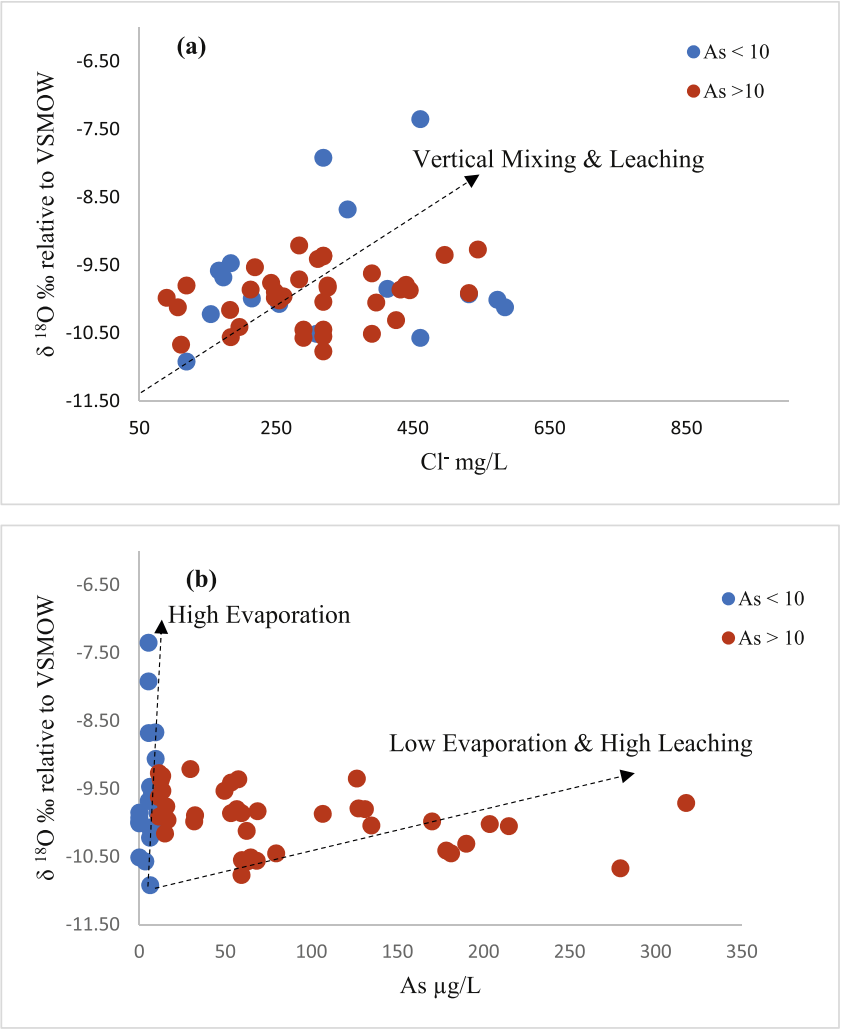

Fig. 8. Plot (a), $\delta^{18}O$ versus chloride with an arsenic concentration in groundwater of present study that indicating leaching and vertical mixing is major process for arsenic mobilization in aquifers, (b) $\delta^{18}O$ versus As concentration in groundwater of present study indicating low evaporation and high leaching process that control arsenic mobilization in aquifers.

Dokri. The graph between $\delta^{18}O$ and Cl^- further supports that fast leaching and vertical mixing with return irrigation water were the ontrolling factors that enhanced the As contamination in the study area. This urgently needs to change the irrigation practices in the area to further reduce the As problem.

Conflicts of interest

The authors have no conflict of interest.

Acknowledgements

The authors are thankful to Dr. Azhar Mashiatullah, Dr. Ume -e-Robab, Dr. Javeria Khalid, and Dr. Nadeem Yaqoob. Isotopic Application Division (IAD) laboratory, Pakistan Institute of Nuclear Science and Technology (PINSTECH), for providing laboratory assistance.

Appendix A. Supplementary data

Supplementary data to this article can be found online at https://doi.org/10.1016/j.envpol.2018.10.103.

References

Ali, W., Rasool, A., Junaid, M., Zhang, H., 2018. A comprehensive review on current status, mechanism, and possible sources of arsenic contamination in groundwater: a global perspective with prominence of Pakistan scenario. Environ. Geochem. Health 1–24.

APHA, 2005. In: American Public Health Association. Standard Methods for the Examination of Water and Wastewater, twenty-first ed. American Public Health Association, Washington DC, p. 1220.

Arain, M., Kazi, T., Baig, J., Jamali, M., Afridi, H., Shah, A., Jalbani, N., Sarfraz, R., 2009. Determination of arsenic levels in lake water, sediment, and foodstuff from selected area of Sindh, Pakistan: estimation of daily dietary intake. Food Chem. Toxicol. 47, 242–248.

Aziz Hasan, M., Bhattacharya, P., Sracek, O., Ahmed, K.M., von Brömssen, M., Jacks, G., 2009. Geological controls on groundwater chemistry and arsenic mobilization: hydrogeochemical study along an EW transect in the Meghna basin, Bangladesh. J. Hydrol. 378, 105–118.

Baig, J.A., Kazi, T.G., Shah, A.Q., Afridi, H.I., Kandhro, G.A., Khan, S., Kolachi, N.F., Wadhwa, S.K., Shah, F., Arain, M.B., 2011. Evaluation of arsenic levels in grain crops samples, irrigated by tube well and canal water. Food Chem. Toxicol. 49, 265–270.

Bowell, R.J., Alpers, C.N., Jamieson, H.E., Nordstrom, D.K., Majzlan, J., 2014. The environmental geochemistry of arsenic—an overview—. Rev. Mineral. Geochem. 79, 1–16.

Brahman, K.D., Kazi, T.G., Afridi, H.I., Naseem, S., Arain, S.S., Ullah, N., 2013. Evaluation of high levels of fluoride, arsenic species and other physicochemical parameters in underground water of two sub districts of Tharparkar, Pakistan: a multivariate study. Water Res. 47, 1005–1020.

Brammer, H., Ravenscroft, P., 2009. Arsenic in groundwater: a threat to sustainable

agriculture in South and South-east Asia. Environ. Int. 35, 647–654.
Buschmann, J., Berg, M., Stengel, C., Sampson, M.L., 2007. Arsenic and manganese contamination of drinking water resources in Cambodia: coincidence of risk areas with low relief topography. Environ. Sci. Technol. 41, 2146–2152.
CENSUS, 2017. Province Wise Provisional Results of Census - 2017.
Chadha, D., Ray, S., 1999. High Incidence of Arsenic in Groundwater in West Bengal. CGWB, Ministry of Water Resources, Faridabad, India.
Chandio, N., Anwar, M., 2009. Impacts of Climate on Agriculture And It's Causes: A Case Study of Taluka Kamber, Sindh, Pakistan, 41. Sindh University Research Journal-SURJ (Science Series).
Choudhury, R., Sharma, P., Mahanta, C., Sharma, H.P., 2015. Evaluation of the processes controlling arsenic contamination in parts of the Brahmaputra floodplains in Assam, India. Environmental Earth Sciences 73, 4473–4482.
Clark, I.D., Fritz, P., 1997. Environmental Isotopes in Hydrogeology. CRC press.
Deutsch, C.V., Journel, A., 1998. Geostatistical Software Library and User's Guide. Oxford University Press, New York.
Ekwere, A.S., Edet, A.E., Ekwere, S.J., 2012. Groundwater chemistry of the oban Massif, south-eastern Nigeria. Revista Ambiente & Água 7, 51–66.
Eqani, S.A.M.A.S., Bhowmik, A.K., Qamar, S., Shah, S.T.A., Sohail, M., Mulla, S.I., Fasola, M., Shen, H., 2016. Mercury contamination in deposited dust and its bioaccumulation patterns throughout Pakistan. Sci. Total Environ. 569, 585–593.
Farooqi, A., Masuda, H., Firdous, N., 2007a. Toxic fluoride and arsenic contaminated groundwater in the Lahore and Kasur districts, Punjab, Pakistan and possible contaminant sources. Environ. Pollut. 145, 839–849.
Farooqi, A., Masuda, H., Kusakabe, M., Naseem, M., Firdous, N., 2007b. Distribution of highly arsenic and fluoride contaminated groundwater from east Punjab, Pakistan, and the controlling role of anthropogenic pollutants in the natural hydrological cycle. Geochem. J. 41, 213–234.
Gat, J.R., 1996. Oxygen and hydrogen isotopes in the hydrologic cycle. Annu. Rev. Earth Planet Sci. 24, 225–262.
Gibbs, R.J., 1970. Mechanisms controlling world water chemistry. Science 170, 1088–1090.
Grynkiewicz, M., Polkowska, Z., Zygmunt, B., Namiesnik, J., 2003. Atmospheric precipitation sampling for analysis. Pol. J. Environ. Stud. 12.
Haque, I.U., Nabi, D., Baig, M., Hayat, W., Trefry, M., 2008. Groundwater Arsenic Contamination–A Multi-Directional Emerging Threat to Water Scarce Areas of Pakistan, 324. IAHS publication, p. 24.
Hassan, K.M., Fukuhara, T., Hai, F.I., Bari, Q.H., Islam, K.M.S., 2009. Development of a bio-physicochemical technique for arsenic removal from groundwater. Desalination 249, 224–229.
Hem, J.D., 1972. Chemistry and occurrence of cadmium and zinc in surface water and groundwater. Water Resour. Res. 8, 661–679.
Huq, M.E., Su, C., Li, J., Sarven, M.S., 2018. Arsenic enrichment and mobilization in the Holocene alluvial aquifers of Prayagpur of Southwestern Bangladesh. Int. Biodeterior. Biodegrad. 128, 186–194.
Katz, B.G., Coplen, T.B., Bullen, T.D., Davis, J.H., 1997. Use of chemical and isotopic tracers to characterize the interactions between ground water and surface water in mantled karst. Ground Water 35, 1014–1028.
Kelly, W.R., Holm, T.R., Wilson, S.D., Roadcap, G.S., 2005. Arsenic in glacial aquifers: sources and geochemical controls. Ground Water 43, 500–510.
Malana, M.A., Khosa, M.A., 2011. Groundwater pollution with special focus on arsenic, Dera Ghazi Khan-Pakistan. Journal of Saudi Chemical Society 15, 39–47.
Mandal, B.K., Suzuki, K.T., 2002. Arsenic round the world: a review. Talanta 58, 201–235.
Mayo, A.L., Loucks, M.D., 1995. Solute and isotopic geochemistry and ground water flow in the central Wasatch Range, Utah. J. Hydrol. 172, 31–59.
McArthur, J., Ravenscroft, P., Banerjee, D., Milsom, J., Hudson-Edwards, K.A., Sengupta, S., Bristow, C., Sarkar, A., Tonkin, S., Purohit, R., 2008. How paleosols influence groundwater flow and arsenic pollution: a model from the Bengal Basin and its worldwide implication. Water Resour. Res. 44.
Mladenov, N., Wolski, P., Hettiarachchi, G.M., Murray-Hudson, M., Enriquez, H., Damaraju, S., Galkaduwa, M.B., McKnight, D.M., Masamba, W., 2014. Abiotic and biotic factors influencing the mobility of arsenic in groundwater of a throughflow island in the Okavango Delta, Botswana. J. Hydrol. 518, 326–341.
Moharir, A., Ramteke, D., Moghe, C., Wate, S., Sarin, R., 2002. Surface and groundwater quality assessment in Bina region. Indian J. Environ. Protect. 22, 961–969.
Mukherjee, A., Bhattacharya, P., Savage, K., Foster, A., Bundschuh, J., 2008. Distribution of Geogenic Arsenic in Hydrologic Systems: Controls and Challenges. Elsevier.
Mukherjee, A., Fryar, A.E., Rowe, H.D., 2007. Regional-scale stable isotopic signatures of recharge and deep groundwater in the arsenic affected areas of West Bengal, India. J. Hydrol. 334, 151–161.
Mushtaq, N., Younas, A., Mashiatullah, A., Javed, T., Ahmad, A., Farooqi, A., 2018. Hydrogeochemical and isotopic evaluation of groundwater with elevated arsenic in alkaline aquifers in Eastern Punjab, Pakistan. Chemosphere 200, 576–586.
Naseem, S., McArthur, J.M., 2018. Arsenic and other water-quality issues affecting groundwater, I ndus alluvial plain, P akistan. Hydrol. Process. 32, 1235–1253.
Nath, B., Berner, Z., Chatterjee, D., Mallik, S.B., Stüben, D., 2008a. Mobility of arsenic in West Bengal aquifers conducting low and high groundwater arsenic. Part II: comparative geochemical profile and leaching study. Appl. Geochem. 23, 996–1011.
Nath, B., Stüben, D., Mallik, S.B., Chatterjee, D., Charlet, L., 2008b. Mobility of arsenic in West Bengal aquifers conducting low and high groundwater arsenic. Part I: comparative hydrochemical and hydrogeological characteristics. Appl. Geochem. 23, 977–995.
Nickson, R., McArthur, J., Ravenscroft, P., Burgess, W., Ahmed, K., 2000. Mechanism of arsenic release to groundwater, Bangladesh and West Bengal. Appl. Geochem. 15, 403–413.
Nickson, R., McArthur, J., Shrestha, B., Kyaw-Myint, T., Lowry, D., 2005. Arsenic and other drinking water quality issues, Muzaffargarh District, Pakistan. Appl. Geochem. 20, 55–68.
Nordstrom, D.K., Wilde, F.D., 2005. Chapter A6. Section 6.5. Reduction-Oxidation Potential (Electrode Method). Geological Survey (US).
Pi, K., Wang, Y., Postma, D., Ma, T., Su, C., Xie, X., 2018. Vertical variability of arsenic concentrations under the control of iron-sulfur-arsenic interactions in reducing aquifer systems. J. Hydrol. 561, 200–210.
Qureshi, A.S., McCornick, P.G., Qadir, M., Aslam, Z., 2008. Managing salinity and waterlogging in the Indus basin of Pakistan. Agric. Water Manag. 95, 1–10.
Rabbani, U., Mahar, G., Siddique, A., Fatmi, Z., 2017. Risk assessment for arsenic-contaminated groundwater along River Indus in Pakistan. Environ. Geochem. Health 39, 179–190.
Rafique, T., Naseem, S., Usmani, T.H., Bashir, E., Khan, F.A., Bhanger, M.I., 2009. Geochemical factors controlling the occurrence of high fluoride groundwater in the Nagar Parkar area, Sindh, Pakistan. J. Hazard Mater. 171, 424–430.
Rahman, A., Lee, H., Khan, M.A., 1997. Domestic water contamination in rapidly growing megacities of Asia: case of Karachi, Pakistan. Environ. Monit. Assess. 44, 339–360.
Rasool, A., Farooqi, A., Masood, S., Hussain, K., 2016. Arsenic in groundwater and its health risk assessment in drinking water of Mailsi, Punjab, Pakistan. Hum. Ecol. Risk Assess. 22, 187–202.
Rehman, A., Asghar, H., Hamid, A., Almas, A.S., Tabassum, M., Yousaf, K., 1998. Waterlogging and Salinity Management in the Sindh Province. Pakistan N Ational Programme. International Irrigation Management I nstitute, December.
Routh, J., Saraswathy, A., 2004. Microbial processes and arsenic mobilization in mine tailings and shallow aquifers. In: Natural Arsenic in Groundwater: Proceedings of the Pre-Congress Workshop" Natural Arsenic in Groundwater", 32nd International Geological Congress, Florence, Italy, 18-19 August 2004. CRC Press, p. 145.
Saunders, J., Lee, M.K., Uddin, A., Mohammad, S., Wilkin, R.T., Fayek, M., Korte, N.E., 2005. Natural arsenic contamination of Holocene alluvial aquifers by linked tectonic, weathering, and microbial processes. G-cubed 6.
Shakoor, M.B., Bibi, I., Niazi, N.K., Shahid, M., Nawaz, M.F., Farooqi, A., Naidu, R., Rahman, M.M., Murtaza, G., Lüttge, A., 2018. The evaluation of arsenic contamination potential, speciation and hydrogeochemical behaviour in aquifers of Punjab, Pakistan. Chemosphere 199, 737–746.
Sheikhy Narany, T., Ramli, M.F., Aris, A.Z., Sulaiman, W.N.A., Juahir, H., Fakharian, K., 2014. Identification of the hydrogeochemical processes in groundwater using classic integrated geochemical methods and geostatistical techniques. In: Amol-babol Plain. The Scientific World Journal, Iran, 2014.
Tabassum, R.A., Shahid, M., Dumat, C., Niazi, N.K., Khalid, S., Shah, N.S., Imran, M., Khalid, S., 2018. Health risk assessment of drinking arsenic-containing groundwater in Hasilpur, Pakistan: effect of sampling area, depth, and source. Environ. Sci. Pollut. Control Ser. 1–12.
Vega, M.A., Kulkarni, H.V., Mladenov, N., Johannesson, K., Hettiarachchi, G.M., Bhattacharya, P., Kumar, N., Weeks, J., Galkaduwa, M., Datta, S., 2017. Biogeochemical controls on the release and accumulation of Mn and as in shallow aquifers, West Bengal, India. Frontiers in Environmental Science 5, 29.
Wagan, M.R., Rajpan, I., Keervo, M.I., Yousifzai, A.A., 2002. Salanity problem in taluka Ratodero district larkana, Sindh Pakistan. Pakistan J. Appl. Sci. 2 (7), 719–722.
Woo, N., Choi, M., 2001. Arsenic and metal contamination of water resources from mining wastes in Korea. Environ. Geol. 40, 305–311.
Xiao, Z., Xie, X., Pi, K., Yan, Y., Li, J., Chi, Z., Qian, K., Wang, Y., 2018. Effects of irrigation-induced water table fluctuation on arsenic mobilization in the unsaturated zone of the Datong Basin, northern China. J. Hydrol. 564, 256–265.
Xie, X., Wang, Y., Su, C., Li, J., Li, M., 2012. Influence of irrigation practices on arsenic mobilization: evidence from isotope composition and Cl/Br ratios in groundwater from Datong Basin, northern China. J. Hydrol. 424, 37–47.
Yeh, H.-F., Lin, H.-I., Lee, C.-H., Hsu, K.-C., Wu, C.-S., 2014. Identifying seasonal groundwater recharge using environmental stable isotopes. Water 6, 2849–2861.
Zheng, Y., Stute, M., Van Geen, A., Gavrieli, I., Dhar, R., Simpson, H., Schlosser, P., Ahmed, K., 2004. Redox control of arsenic mobilization in Bangladesh groundwater. Appl. Geochem. 19, 201–214.
Zhu, G., Li, Z., Su, Y., Ma, J., Zhang, Y., 2007. Hydrogeochemical and isotope evidence of groundwater evolution and recharge in Minqin Basin, Northwest China. J. Hydrol. 333, 239–251.
Zhu, J., Lou, Z., Liu, Y., Fu, R., Baig, S.A., Xu, X., 2015. Adsorption behavior and removal mechanism of arsenic on graphene modified by iron–manganese binary oxide (FeMnO x/RGO) from aqueous solutions. RSC Adv. 5, 67951–67961.